PAPER • OPEN ACCESS
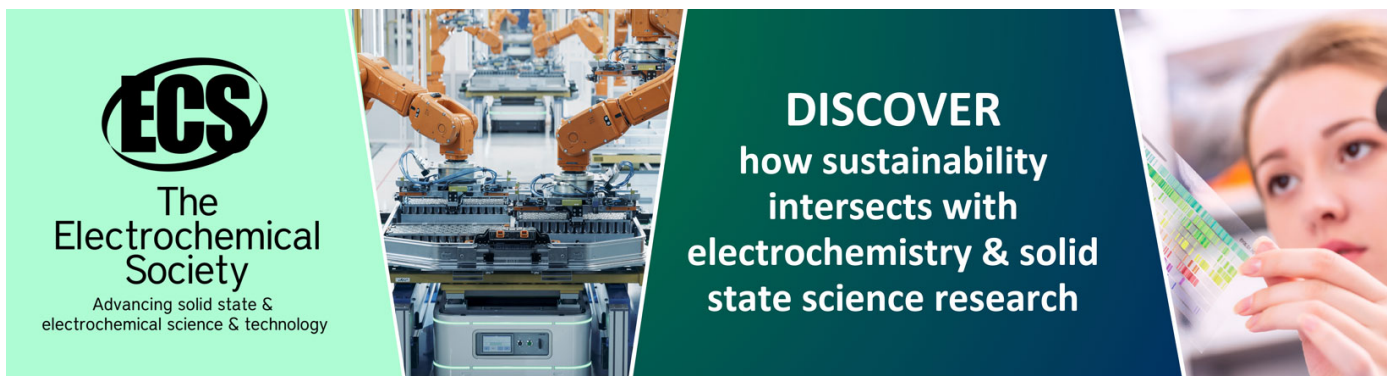
KLEVER: An experiment to measure BR($K_L \to \pi^0 \nu \bar{\nu}$) at the CERN SPS

To cite this article: M Moulson and for the KLEVER Project 2020 *J. Phys.: Conf. Ser.* **1526** 012028

View the article online for updates and enhancements.

KLEVER: An experiment to measure BR($K_L \to \pi^0 \nu\bar{\nu}$) at the CERN SPS

M Moulson, for the KLEVER Project[1]

INFN Laboratori Nazionali di Frascati, 00044 Frascati RM, Italy

E-mail: moulson@lnf.infn.it

Abstract. Precise measurements of the branching ratios for the flavor-changing neutral current decays $K \to \pi\nu\bar{\nu}$ can provide unique constraints on CKM unitarity and, potentially, evidence for new physics. It is important to measure both decay modes, $K^+ \to \pi^+\nu\bar{\nu}$ and $K_L \to \pi^0\nu\bar{\nu}$, since different new physics models affect the rates for each channel differently. The NA62 experiment at the CERN SPS will measure the BR for the charged channel to better than 20%. The BR for the neutral channel has never been measured. We are designing the KLEVER experiment to measure BR($K_L \to \pi^0\nu\bar{\nu}$) to ∼20% using a high-energy neutral beam at the CERN SPS. The boost from the high-energy beam facilitates the rejection of background channels such as $K_L \to \pi^0\pi^0$ by detection of the additional photons in the final state. On the other hand, the layout poses particular challenges for the design of the small-angle vetoes, which must reject photons from K_L decays escaping through the beam exit amid an intense background from soft photons and neutrons in the beam. We present findings from our design studies, with an emphasis on the challenges faced and the potential sensitivity for the measurement of BR($K_L \to \pi^0\nu\bar{\nu}$).

1. Introduction

The branching ratios (BRs) for the decays $K \to \pi\nu\bar{\nu}$ are among the observables in the quark flavor sector most sensitive to new physics. The Standard Model (SM) rates for these flavor-changing neutral-current decays are very strongly suppressed by the GIM mechanism and the CKM hierarchy. In addition, because of the dominance of the diagrams with top loops, the lack of contributions from intermediate photons, and the fact that the hadronic matrix element can be obtained from K_{e3} data, the SM rates can be calculated very precisely: BR($K^+ \to \pi^+\nu\bar{\nu}$) = $(8.4 \pm 1.0) \times 10^{-11}$ and BR($K_L \to \pi^0\nu\bar{\nu}$) = $(3.4 \pm 0.6) \times 10^{-11}$, where the uncertainties are dominated by the external contributions from V_{cb} and V_{ub} and the non-parametric theoretical uncertainties are about 3.5% and 1.5%, respectively [1].

[1] The KLEVER Project: F Ambrosino, R Ammendola, A Antonelli, K Ayers, D Badoni, G Ballerini, L Bandiera, J Bernhard, C Biino, L Bomben, V Bonaiuto, A Bradley, M B Brunetti, F Bucci, A Cassese, R Camattari, M Corvino, D De Salvador, D Di Filippo, M van Dijk, N Doble, R Fantechi, S Fedotov, A Filippi, F Fontana, L Gatignon, G Georgiev, A Gerbershagen, A Gianoli, E Imbergamo, K Kampf, M Khabibullin, S Kholodenko, A Khotjantsev, V Kozhuharov, Y Kudenko, V Kurochka, G Lamanna, M Lenti, L Litov, E Lutsenko, T Maiolino, I Mannelli, S Martellotti, M Martini, V Mascagna, A Maslenkina, P Massarotti, A Mazzolari, E Menichetti, O Mineev, M Mirra, M Moulson, I Neri, M Napolitano, V Obraztsov, A Ostankov, G Paoluzzi, F Petrucci, M Prest, M Romagnoni, M Rosenthal, P Rubin, A Salamon, G Salina, F Sargeni, A Shaykhiev, A Smirnov, M Soldani, D Soldi, M Sozzi, V Sugoniaev, A Sytov, E Vallazza, R Volpe, R Wanke, N Yershov

Because these decays are strongly suppressed and calculated very precisely in the SM, their BRs are potentially sensitive to mass scales of hundreds of TeV, surpassing the sensitivity of B decays in most SM extensions [2]. Observations of lepton-flavor-universality-violating phenomena are mounting in the B sector [3]. Most explanations for such phenomena predict strong third-generation couplings and thus significant changes to the $K \to \pi\nu\bar\nu$ BRs through couplings to final states with τ neutrinos [4]. Measurements of the $K \to \pi\nu\bar\nu$ BRs are critical to interpreting the data from rare B decays, and may demonstrate that these effects are a manifestation of new degrees of freedom such as leptoquarks [5, 6]. Because the amplitude for $K^+ \to \pi^+\nu\bar\nu$ has both real and imaginary parts, while the amplitude for $K_L \to \pi^0\nu\bar\nu$ is purely imaginary, the two decays have different sensitivity to new sources of CP violation. Measurements of both BRs would therefore be extremely useful not only to uncover evidence of new physics in the quark-flavor sector, but also to distinguish between new physics models.

The BR for the charged decay $K^+ \to \pi^+\nu\bar\nu$ was first measured by Brookhaven experiment E787 and its successor, E949, using K^+ decays at rest [7]. The NA62 experiment at the CERN SPS has recently obtained a stronger constraint on the BR using decay-in-flight data collected in 2016–2017. The preliminary NA62 result is $\mathrm{BR}(K^+ \to \pi^+\nu\bar\nu) < 24.4 \times 10^{-11}$ (95% CL), with a single-event sensitivity (SES) of $(3.46 \pm 0.17) \times 10^{-11}$, 1.65 ± 0.31 expected background events, and three observed signal candidates [8]. Additional running is contemplated beginning in 2021, with the goal of measuring the BR to 20% precision or better [9].

The decay $K_L \to \pi^0\nu\bar\nu$ has never been measured, and the KOTO experiment at J-PARC is the only experiment currently pursuing its observation. The salient features of the KOTO experiment are the use of a highly collimated, low-energy (mean momentum 2.1 GeV) "pencil" beam and very-high-performance hermetic calorimetry and photon vetoing. From an analysis of 2015 data, KOTO has recently obtained the limit $\mathrm{BR}(K_L \to \pi^0\nu\bar\nu) < 3.0 \times 10^{-9}$ (90% CL), with an expected background of 0.42 ± 0.18 events and no candidate events observed [10]. More recently, in a preliminary analysis of data collected in 2016–2018, the experiment has achieved an SES of 6.9×10^{-10} with 0.05 ± 0.02 background events expected. Four events found in the signal region are under further investigation [11]. KOTO should reach an SES equal to the SM BR for the decay by the mid 2020s, and upgrades to the experiment planned or in progress should reduce backgrounds by a similar factor [12]. This would allow a 90% CL upper limit on the BR to be set at the 10^{-10} level, but a next-generation experiment is needed in order to actually measure the BR.

2. KLEVER

We are designing the KLEVER experiment to use a high-energy neutral beam at the CERN SPS to achieve a sensitivity of about 60 events for the decay $K_L \to \pi^0\nu\bar\nu$ at the SM BR with an S/B ratio of 1. At the SM BR, this would correspond to a relative uncertainty of about 20%. We would expect to observe a discrepancy with 5σ significance if the true rate is a bit more than twice or less than one-quarter of the SM rate, or with 3σ significance if the true rate is less than half of the SM rate. These scenarios are consistent with the rates predicted for many different SM extensions [13].

The KLEVER timescale is driven by the assumption that the multi-decade North Area program in kaon physics, building on the successes of NA62 and its progenitors, will have advanced by the end of LHC Run 3 to the point at which the measurement of $K_L \to \pi^0\nu\bar\nu$ is the natural next step. KLEVER would aim to start data taking in LHC Run 4 (2026). The layout is sketched in Figure 1. Relative to KOTO, the boost from the high-energy beam in KLEVER facilitates the rejection of background channels such as $K_L \to \pi^0\pi^0$ by detection of the additional photons in the final state. On the other hand, the layout poses particular challenges for the design of the small-angle vetoes, which must reject photons from K_L decays escaping through the beam exit amidst an intense background from soft photons and neutrons
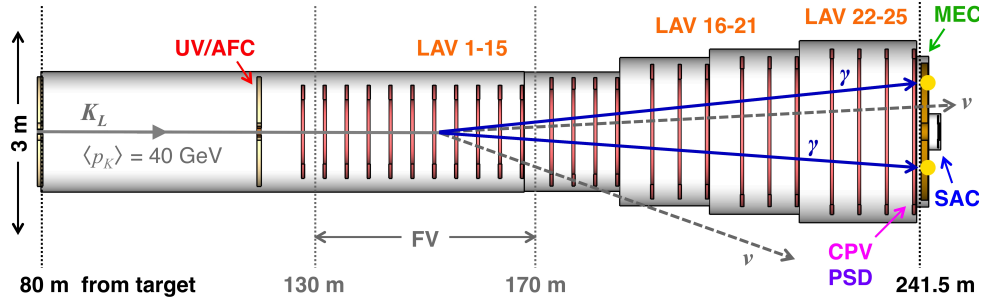
Figure 1. KLEVER experimental apparatus: upstream veto (UV) and active final collimator (AFC), large-angle photon vetoes (LAV), main electromagnetic calorimeter (MEC), small-angle calorimeter (SAC), charged particle veto (CPV), preshower detector (PSD).

in the beam. Background from $\Lambda \to n\pi^0$ decays in the beam must also be kept under control.

2.1. Beam

KLEVER will make use of the 400-GeV SPS proton beam to produce a neutral secondary beam at an angle of 8 mrad with an opening angle of 0.4 mrad. The choice of production angle balances increased K_L production and higher K_L momentum at small angle with improved K_L/n and K_L/Λ ratios at larger angles. The choice of solid angle balances beam flux against the need for tight collimation for increased $p_\perp$ constraints to reject the main background from $K_L \to \pi^0\pi^0$ with lost photons. The resulting neutral beam has a mean K_L momentum of 40 GeV, leading to an acceptance of 4% for the fiducial volume extending from 130 to 170 m downstream of the target, and a K_L yield of 2×10^{-5} K_L per proton on target (pot). With a selection efficiency of 5%, collection of 60 SM events would require a total primary flux of 5×10^{19} pot, corresponding to an intensity of 2×10^{13} protons per pulse (ppp) under NA62-like slow-extraction conditions, with a 16.8 s spill cycle and 100 effective days of running per year. This is a six-fold increase in the primary intensity relative to NA62. The feasibility of upgrades to the P42 beamline, TCC8 target gallery, and ECN3 experimental cavern to handle this intensity has been studied by the Conventional Beams working group in the context of the Physics Beyond Colliders initiative, and preliminary indications are positive [14, 15].

A four-collimator neutral beamline layout for ECN3 has been developed, as illustrated in Fig. 2. The primary proton beam, sloping downwards at an angle of 8 mrad, is incident on the T10 target (assumed to be a beryllium rod of 2 mm radius), producing the neutral beam and other secondaries. This is immediately followed by a vertical sweeping magnet that bends the protons further downward by 5.6 mrad, and a TAX dump collimator with a hole for the passage of the neutral beam. A horizontal sweeping magnet downstream of the TAX reduces the background further. A collimator at $z = 40$ m downstream of the target with $r = 16$ mm defines the beam solid angle, and a cleaning collimator at $z = 80$ m removes halo from particles interacting on the edges of the defining collimator. Both are followed by horizontal sweeping magnets. The sweeping fields have been optimized to minimize muon backgrounds. The final stage of collimation is the active final collimator (AFC) incorporated into the upstream veto (UV) at $z = 120$ m. The cleaning and final (AFC) collimators have apertures which are progressively larger than the beam acceptance, such that the former lies outside a cone from the (2 mm radius) target passing through the defining collimator, and the latter lies outside a cone from the TAX aperture passing through the cleaning collimator. The design of the beamline has been guided by FLUKA and Geant4 simulations to quantify the extent and composition of beam halo, muon backgrounds, and sweeping requirements. According to the simulations, for an intensity of 2×10^{13} ppp and an effective spill length of 3 s, there are 140 MHz of K_L in
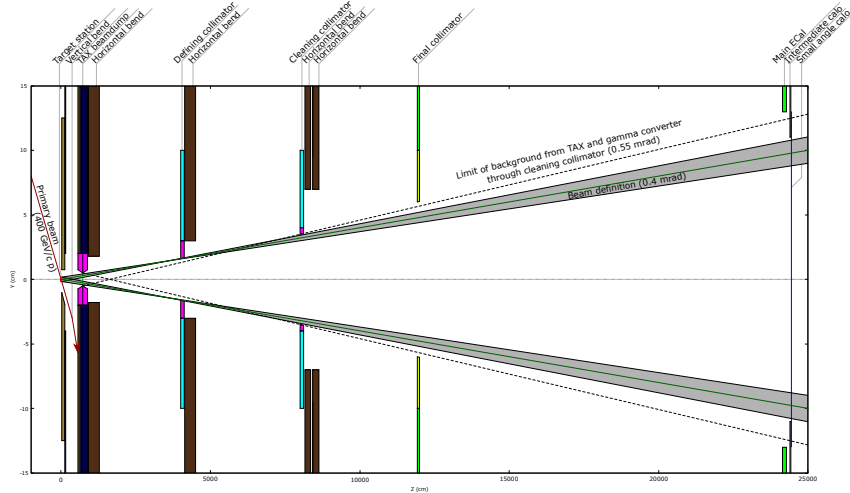
Figure 2. KLEVER neutral beamline layout as modeled in FLUKA, showing four collimation stages corresponding to dump, defining, cleaning, and final collimators. The final collimator is an active detector (AFC), built into the upstream veto. The aperture of the main calorimeter and coverage of the small-angle calorimeters is also shown.

the beam and 440 MHz of neutrons [16]. An oriented tungsten crystal in the center of the TAX converts the vast majority of the photons in the beam into e^+e^- pairs, which are swept away, but 40 MHz of photons with energy greater than 5 GeV remain. As noted below, the use of an oriented crystal converter maximizes the transparency to neutral hadrons at a given thickness in radiation lengths ($9.4X_0$).

2.2. Detector
Because of the experimental challenges involved in the measurement of $K_L \to \pi^0 \nu \bar{\nu}$, and in particular, the very high efficiency required for the photon veto systems, most of the subdetector systems for KLEVER will have to be newly constructed.

Main electromagnetic calorimeter (MEC)   Early studies indicated that the NA48 liquid-krypton calorimeter (LKr) [17] currently used in NA62 could be reused as the MEC for reconstruction of the π^0 for signal events and rejection of events with additional photons. Indeed, the efficiency and energy resolution of the LKr appear to be satisfactory for KLEVER. However, the LKr time resolution would be a major liability. The LKr would measure the event time in KLEVER with 500 ps resolution, while the total rate of accidental vetoes (dominated by the rate from beam photons interacting in the SAC) could be 100 MHz. The LKr time resolution might be improved via a comprehensive readout upgrade, but concerns about the service life of the LKr would remain, and the size of the inner bore would limit the beam solid angle and hence kaon flux.

We are investigating the possibility of replacing the LKr with a shashlyk-based MEC patterned on the PANDA FS calorimeter (in turn, based on the KOPIO calorimeter [18]), with 110×110 mm modules, lead absorber thickness of 0.275 mm, and scintillator thickness of 1.5 mm, read out by silicon photomultipliers via 1-mm diameter WLS fibers. Stochastic energy and time resolutions of better than $\sigma_E/E = 2\%/\sqrt{E}$ and $\sigma_t = 72$ ps$/\sqrt{E}$ were obtained with this design in KOPIO tests. We envisage a shashlyk design incorporating "spy tiles", consisting of 10-mm thick scintillator bricks incorporated into the shashlyk stack but optically isolated from it and read out by separate WLS fibers. The spy tiles are located at key points in the

longitudinal shower development: near the front of the stack, near shower maximum, and in the shower tail. This provides longitudinal sampling of the shower development, resulting in additional information for γ/n separation. A first test of this concept was carried out with a prototype detector at Protvino in April 2018.

Upstream veto (UV) and active final collimator (AFC)   The upstream veto (UV) rejects $K_L \to \pi^0\pi^0$ decays in the 40 m upstream of the fiducial volume where there are no large-angle photon vetoes. The UV is a shashlyk calorimeter with the same basic structure as the MEC (without the spy tiles).

The active final collimator (AFC) is inserted into a 100-mm hole in center of the UV. The AFC is a LYSO collar counter with angled inner surfaces to provide the last stage of beam collimation while vetoing photons from K_L that decay in transit through the collimator itself. The collar is made of 24 crystals of trapezoidal cross section, forming a detector with an inner radius of 60 mm. The UV and AFC are both 800 mm in depth. The maximum crystal length for a practical AFC design is about 250 mm, so the detector consists of 3 or 4 longitudinal segments. The crystals are read out on the back side with two avalanche photodiodes (APDs). These devices couple well with LYSO and offer high quantum efficiency and simple signal and HV management. Studies indicate that a light yield in excess of 4000 p.e./MeV should be easy to achieve.

Large-angle photon vetoes   Because of the boost from the high-energy beam, it is sufficient for the large-angle photon vetoes (LAVs) to cover polar angles out to 100 mrad. The detectors themselves must have inefficiencies of less than a few 10^{-4} down to at least 100 MeV, so the current NA62 LAVs based on the OPAL lead glass cannot be reused [19] The 25 new LAV detectors for KLEVER are lead/scintillating-tile sampling calorimeters with wavelength-shifting fiber readout, based on the CKM VVS design [20]. Extensive experience with this type of detector (including in prototype tests for NA62) demonstrates that the low-energy photon detection efficiency will be sufficient for KLEVER [21, 22, 23].

Small-angle calorimeter   The small-angle calorimeter (SAC) sits directly in the neutral beam and must reject photons from K_L decays that would otherwise escape via the downstream beam exit. The veto efficiency required is not intrinsically daunting (inefficiency $< 1\%$ for 5 GeV $< E_\gamma < 30$ GeV and $< 10^{-4}$ for $E_\gamma > 30$ GeV; the SAC can be blind for $E_\gamma < 5$ GeV), but must be attained while maintaining insensitivity to more than 500 MHz of neutral hadrons in the beam. In addition, the SAC must have good longitudinal and transverse segmentation to provide γ/n discrimination. In order to keep the false veto rate from accidental coincidence of beam neutrons to an acceptable level (< 10 MHz), and assuming that about 25% of the beam neutrons leave signals above threshold in the SAC, topological information from the SAC must allow residual neutron interactions to be identified with 90% efficiency while maintaining 99% detection efficiency for photons with $E_\gamma > 5$ GeV.

An intriguing possibility for the construction of an instrument that is sensitive to photons and blind to hadrons is to use a compact Si-W sampling calorimeter with crystalline tungsten tiles as the absorber material, since coherent interactions of high-energy photons with a crystal lattice can lead to increased rates of pair conversion relative to those obtained with amorphous materials [24, 25, 26]. The effect is dependent on photon energy and incident angle; in the case of KLEVER, one might hope to decrease the ratio $X_0/\lambda_{\rm int}$ by a factor of 2–3. The same effect could be used to efficiently convert high-energy photons in the neutral beam to e^+e^- pairs at the TAX for subsequent sweeping, thereby allowing the use of a thinner converter to minimize the scattering of hadrons from the beam. Both concepts were tested in summer 2018 in the SPS H2 beam line, in a joint effort together with the AXIAL collaboration. In these tests, a

beam of tagged photons with energies of up to 80 GeV was obtained from a 120-GeV electron beam; interactions of the beam with crystalline tungsten samples of 2 mm and 10 mm thick were studied as a function of photon energy and angle of incidence with detectors just downstream of the samples to measure charged multiplicity and forward energy. While the data are still under analysis, the initial results show a significant increase for both samples in the probability for electromagnetic interactions when the crystal axis is aligned with the beam, corresponding to the expected shortening of the radiation length, with a somewhat smaller effect in the (lower-quality) thicker crystal counterbalanced by a larger angular range over which the effect is observed (a few mrad vs. about 1 mrad).

Charged-particle rejection   For the rejection of charged particles, K_{e3} is a benchmark channel because of its large BR and because the final state electron can be mistaken for a photon. Simulations indicate that the needed rejection can be achieved with two planes of charged-particle veto (CPV) each providing 99.5% detection efficiency, supplemented by the $\mu^{\pm}$ and $\pi^{\pm}$ recognition capabilities of the MEC (assumed in this case to be equal to those of the LKr) and the current NA62 hadronic calorimeters and muon vetoes, which could be reused in KLEVER. The CPVs are positioned $\sim$3 m upstream of the MEC and are assumed to be constructed out of thin scintillator tiles. In thicker scintillation hodoscopes, the detection inefficiency arises mainly from the gaps between scintillators. For KLEVER, the scintillators will be only $\sim$5 mm thick (1.2% X_0), and the design will be carefully optimized to avoid insensitive gaps.

Preshower detector   The PSD measures the directions for photons incident on the MEC. Without the PSD, the z-position of the π^0 decay vertex can only be reconstructed by assuming that two clusters on the MEC are indeed photons from the decay of a single π^0. With the PSD, a vertex can be reconstructed by projecting the photon trajectories to the beamline. The invariant mass is then an independent quantity, and $K_L \to \pi^0\pi^0$ decays with mispaired photons can be efficiently rejected. The vertex can be reconstructed using a single photon and the constraint from the nominal beam axis. Simulations show that with $0.5X_0$ of converter (corresponding to a probability of at least one conversion of 50%) and two tracking planes with a spatial resolution of 100 μm, placed 50 cm apart, the mass resolution is about 20 MeV and the vertex position resolution is about 10 m. The tracking detectors must cover a surface of about 5 m^2 with minimal material. Micropattern gas detector (MPGD) technology seems perfectly suited for the PSD. Information from the PSD will be used for bifurcation studies of the background and for the selection of control samples, as well as in signal selection.

2.3. Simulation and performance

Simulations of the experiment carried out with fast-simulation techniques (idealized geometry, parameterized detector response, etc.) show that the target sensitivity is achievable (60 SM events with $S/B = 1$). Background channels considered at high simulation statistics include $K_L \to \pi^0\pi^0$ (including events with reconstructed photons from different π^0s and events with overlapping photons on the MEC), $K_L \to 3\pi^0$, and $K_L \to \gamma\gamma$. Fig. 3 illustrates the scheme for differentiating signal events from $K_L \to \pi^0\pi^0$ background. Events with exactly two photons on the MEC and no other activity in the detector are selected. The clusters on the MEC from both photons must also be more than 35 cm from the beam axis (this helps to increase the rejection for events with overlapping clusters). If one or both photons convert in the PSD, the reconstructed vertex position must be inside the fiducial volume. The plots show the distributions of the events satisfying these minimal criteria in the plane of $p_\perp$ vs. $z_{\rm rec}$ for the π^0, where the distance from the π^0 to the MEC is obtained from the transverse separation of the two photon clusters, assuming that they come from a π^0 ($M_{\gamma\gamma} = m_{\pi^0}$). This scheme is far from final and there is room for improvement with a multivariate analysis, but is does demonstrate that it should be
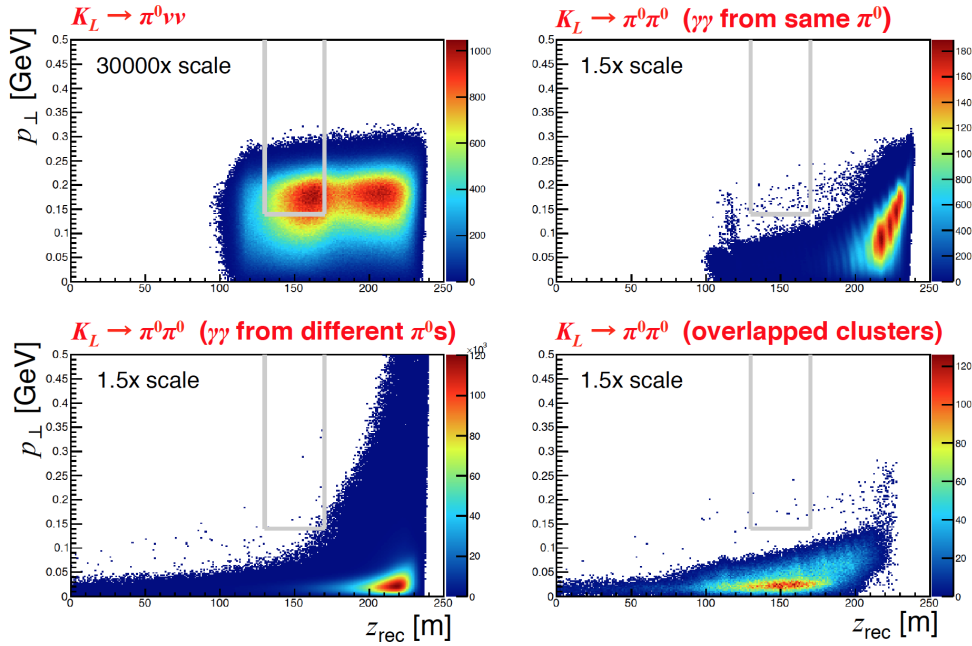
Figure 3. Distributions of events in plane of $(z_{rec}, p_\perp)$ after basic event selection cuts, from fast MC simulation, for $K_L \to \pi^0 \nu \bar{\nu}$ events (top left) and for $K_L \to \pi^0 \pi^0$ events with two photons from the same π^0 (top right), two photons from different π^0s (bottom left), and with two or more indistinguishable overlapping photon clusters (bottom right).

possible to obtain $S/B \sim 1$ with respect to other K_L decays. Background from $\Lambda \to n\pi^0$ and from decays with charged particles is assumed to be eliminated on the basis of studies with more limited statistics. In particular, the background from $\Lambda \to n\pi^0$ is reduced by several orders of magnitude by the 130-m length from the target to the fiducial volume and the choice of production angle, which is carefully optimized to balance K_L flux against the need to keep the Λ momentum spectrum soft. Residual background can then be effectively eliminated by cuts on $p_\perp$ and in the θ vs. p plane for the π^0. The background from single π^0 production in interactions of beam neutrons on residual gas has been estimated to be a most a few percent of the expected signal for a residual gas pressure of 10^{-7} mbar.

An effort is underway to develop a comprehensive simulation and use it to validate the results obtained so far. Of particular note, backgrounds from radiative K_L decays and cascading hyperon decays remain to be studied, and the neutral-beam halo from our detailed FLUKA beamline simulation needs to be fully incorporated into the simulation of the experiment. While mitigation of potential background contributions from one or more of these sources might ultimately require specific modifications to the experimental setup, we expect this task to be less complicated than dealing with the primary challenges from $K_L \to \pi^0\pi^0$ and $\Lambda \to n\pi^0$.

3. Conclusions

Significant progress on the KLEVER design has been made as a part of and with support from the Physics Beyond Colliders initiative at CERN in preparation for the 2020 update of the European Strategy for Particle Physics [13]. The studies described here are preliminary. In particular, high-statistics background studies have been carried out for only a few channels. Some potential backgrounds, such as backgrounds from decays with charged particles emitted in the very forward region, remain to be investigated in detail, and some of the detector concepts require validation. With these caveats, our design studies indicate that an experiment to measure $\text{BR}(K_L \to \pi^0\nu\bar{\nu})$

can be performed at the SPS. An expression of interest to the SPSC is in preparation.

The KLEVER project builds on a CERN tradition of groundbreaking experiments in kaon physics, following on the successes of NA31, NA48, NA48/2, and NA62. Many institutes currently participating in NA62 have expressed support for and interest in the KLEVER project. Successfully carrying out the KLEVER experimental program will require the involvement of new institutions and groups, and we are actively seeking to expand the collaboration at present.

References

[1] Buras A J, Buttazzo D, Girrbach-Noe J and Knegjens R 2015 *JHEP* **1511** 033
[2] Buras A J, Buttazzo D, Girrbach-Noe J and Knegjens R 2014 *JHEP* **1411** 121
[3] Bifani S, Descotes-Genon S, Romero Vidal A and Schune M H arXiv:1809.06229 [hep-ex]
[4] Bordone M, Buttazzo D, Isidori G and Monnard J 2017 *Eur. Phys. J. C* **77** 618
[5] Buttazzo D, Greljo A, Isidori G and Marzocca D 2017 *JHEP* **1711** 044
[6] Fajfer S, Košnik N and Vale Silva L 2018 *Eur. Phys. J. C* **78** 275
[7] Artamonov A V *et al* [BNL-E949 Collaboration] 2009 *Phys. Rev. D* **79** 092004
[8] Ruggiero G these proceedings
[9] NA62 Collaboration 2019 Addendum I to P326: Continuation of the physics programme of the NA62 experiment CERN SPSC-2019-039/SPSC-P-326-ADD-1
[10] Ahn J K *et al* [KOTO Collaboration] 2019 *Phys. Rev. Lett.* **122** 021802
[11] Shinohara S these proceedings
[12] Tung Y C these proceedings
[13] Ambrosino F *et al* [KLEVER Project] 2019 KLEVER-PUB-02, arXiv:1901.03099 [hep-ex]
[14] Banerjee D *et al* [Physics Beyond Colliders Conventional Beams Working Group] 2018 CERN-PBC-NOTES-2018-005
[15] Gatignon L *et al* [Physics Beyond Colliders Conventional Beams Working Group] 2018 CERN-PBC-REPORT-2018-002
[16] van Dijk M and Rosenthal M 2018 CERN-PBC-NOTES-2018-002/CERN-ACC-NOTE-2018-066/KLEVER-PUB-18-01
[17] Fanti V *et al* [NA48 Collaboration] 2007 *Nucl. Instrum. Meth. A* **574** 433
[18] Atoian G S *et al.* 2008 *Nucl. Instrum. Meth. A* **584** 291
[19] Cortina Gil E *et al* [NA62 Collaboration] 2017 *JINST* **1712** P05025
[20] Ramberg E, Cooper P and Tschirhart R 2004 *IEEE Trans. Nucl. Sci.* **51** 2201
[21] Atiya M S 1992 *Nucl. Instrum. Meth. A* **321** 129
[22] Comfort J R *et al* [KOPIO Project] 2015 Conceptual Design Report
[23] Ambrosino F *et al.* 2007 Proceedings, 2007 IEEE Nuclear Science Symposium and Medical Imaging Conference: Honolulu, Hawaii, 28 October-3 November 2007, p. 57-64
[24] Bak J F *et al.* 1988 *Phys. Lett. B* **202** 615
[25] Kimball J C and Cue N 1985 *Phys. Rept.* **125** 69
[26] Baryshevsky V G and Tikhomirov V V 1989 *Sov. Phys. Usp.* **32** 1013 [*Usp. Fiz. Nauk.* **159** (1989) 529]